

Total Reaction and Elastic Scattering Cross Sections for 22.8-Mev Protons on Uranium Isotopes

CLYDE B. FULMER

Oak Ridge National Laboratory,* Oak Ridge, Tennessee

(Received April 16, 1959)

The total reaction cross sections for 22.8-Mev protons on uranium isotopes were determined by measuring cross sections for $(p, \text{fission})$, (p, p') , (p, d) , (p, t) , and (p, α) . These data are combined with previously measured (p, xn) cross sections to give total reaction cross sections of 1.43 ± 0.10 , 1.44 ± 0.10 , and 1.39 ± 0.10 barns for 22.8-Mev protons on U^{233} , U^{235} , and U^{238} , respectively. Angular distributions of (p, p') , (p, d) , (p, t) , (p, α) , and proton elastic scattering cross sections are shown for U^{235} and U^{238} .

INTRODUCTION

THERE exists considerable evidence that neutron, proton, and alpha-particle elastic scattering cross sections are described by the optical model of the nucleus.¹⁻⁴ Numerous sets of experimental data have been successfully fitted by analyses involving proper selection of optical model parameters.²⁻¹⁶ However, sets of parameters are not unique. In particular, it has been shown that if VR^2 (V is the depth of the real part of the nuclear potential, and R is the nuclear radius) is held fixed, the individual parameters can vary over a considerable range of values.

It has been emphasized^{2,4,5,17} that experimental measurements of total reaction cross sections would provide a desirable check on the results of optical model analyses and determine the nuclear radius parameter, R , and hence the real nuclear potential parameter V .

McCormick and Cohen¹⁸ have shown that the fission cross section is almost the total compound nucleus cross section for medium energy protons on uranium isotopes; they determined the (p, xn) cross sections and the $(p, \text{fission})$ cross section for 22-Mev protons on U^{238} with an uncertainty of $\pm 15\%$.

In the work reported here, total reaction cross sections for 22.8-Mev protons on the uranium isotopes U^{233} , U^{235} , and U^{238} were determined by measuring

individual components of the reaction cross section. Elastic scattering cross sections for 22.8-Mev protons on U^{235} and U^{238} were also measured over a large angular range. The former, when compared with results of optical model analyses of the latter, should establish the nuclear radius and the real nuclear potential parameters.

EXPERIMENTAL

The energy-analyzed external proton beam of the ORNL 86-inch cyclotron was used for these experiments. The experimental arrangement used for $(p, \text{fission})$ cross section measurements is shown in Fig. 1. The proton beam is defined by a $\frac{1}{8}$ -in. diam collimator, passes through the target, and is then monitored in a Faraday cup.

The targets used for the fission measurements consist of electroplatings of uranium ~ 1 mg/cm² thick on backings of metallic nickel 0.002-in. thick. The isotopic purities of the targets are U^{233} —98.63 \pm 0.03%, U^{235} —93.18 \pm 0.01%, and U^{238} —99.9997 \pm 0.003%. The targets were prepared by electroplating a surface of several square inches, scanning the surface with a small end-window alpha-particle counter to check for uniformity of uranium thickness, and cutting out $\frac{1}{2}$ -in. square

* Operated for the U. S. Atomic Energy Commission by Union Carbide Corporation.

¹ Feshbach, Porter, and Weisskopf, Phys. Rev. **96**, 448 (1954).

² A. E. Glassgold *et al.*, Phys. Rev. **106**, 1207 (1957).

³ Melkanoff, Nodvik, Saxon, and Woods, Phys. Rev. **106**, 793 (1957).

⁴ G. Igo and R. M. Thaler, Phys. Rev. **106**, 126 (1957).

⁵ A. E. Glassgold and P. J. Kellogg, Phys. Rev. **107**, 1372 (1957).

⁶ A. E. Glassgold and P. J. Kellogg, Phys. Rev. **109**, 1291 (1958).

⁷ Melkanoff, Moszkowski, Nodvik, and Saxon, Phys. Rev. **101**, 507 (1956).

⁸ R. W. Woods and D. S. Saxon, Phys. Rev. **95**, 577 (1954).

⁹ G. Igo, Phys. Rev. Letters **1**, 72 (1958).

¹⁰ W. B. Cheston and A. E. Glassgold, Phys. Rev. **106**, 1215 (1957).

¹¹ Fernbach, Heckrotte, and Lepore, Phys. Rev. **97**, 1059 (1955).

¹² R. M. Sternheimer, Phys. Rev. **97**, 1314 (1955).

¹³ R. M. Sternheimer, Phys. Rev. **100**, 886 (1955).

¹⁴ W. Heckrotte, Phys. Rev. **101**, 1406 (1956).

¹⁵ T. Eriksson, Nuovo cimento **2**, 907 (1955).

¹⁶ S. Kohler, Nuovo cimento **2**, 911 (1955).

¹⁷ N. M. Hintz, Phys. Rev. **106**, 1201 (1957).

¹⁸ G. H. McCormick and B. L. Cohen, Phys. Rev. **96**, 722 (1954).

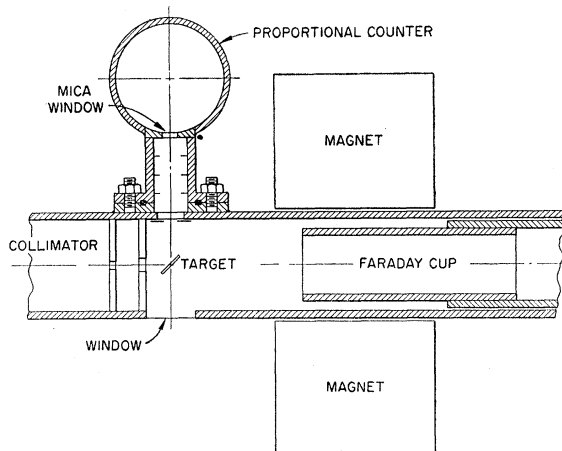


FIG. 1. Experimental arrangement used for $(p, \text{fission})$ cross sections measurements.

specimens of uniform uranium thickness. The uranium thickness of each target was then determined by measuring the specific alpha activity with a 2π counter.¹⁹ The uncertainty of the thicknesses of targets plated with U^{235} and U^{238} is $\pm 1\%$; the uncertainty of the thicknesses of the U^{233} -plated targets is $\pm 5\%$. Several targets of a range of thickness were used; thus a check on the validity of the thickness determinations was provided.

Fission rates are determined by counting the outgoing fission fragments with a 2-in. thick proportional counter which is filled to a pressure of ~ 2 cm Hg with a 90% argon-10% methane gas mixture. The $\frac{1}{4}$ -in. diam mica window (1.6 mg/cm² thick) defines the counter geometry. Antiscattering slits, made of 0.001-in. aluminum foil, prevent fragments scattered by the walls of the assembly from entering the proportional counter. The fission fragments, after escaping from the target and passing through the mica window, have energies of ~ 15 Mev and ~ 30 Mev for the average heavy and light fragments, respectively,²⁰ and thus produce large pulses in the thin proportional counter. Other particles produce smaller pulses that are readily distinguished from the fission-fragment pulses by pulse-height analysis. The target foils are clamped to the end of a metal rod which passes through an O-ring seal to the exterior of the vacuum chamber; thus the target can be rotated while the vacuum is maintained. For checking the validity of a fission-fragment count, the target may be rotated 180 deg so that the detector observes the nickel backing which is opaque to fission fragments, and the detector count repeated. This test was made frequently during the experiments.

Since the fission cross section is a large fraction of the total reaction cross section for 22-Mev protons on uranium, a precision measurement of the former is essential for an accurate determination of the latter. One potentially important source of experimental uncertainty in this type of experiment is the beam current monitoring system. Errors can arise from three sources: (1) ionization of gas molecules, (2) secondary electrons entering or leaving the Faraday cup, and (3) multiple scattering. The permanent magnet (see Fig. 1) maintains a field of ~ 1000 gauss in the region of the Faraday cup entrance. This is sufficient field intensity to "curl up" secondary electrons and prevent them from entering or leaving the Faraday cup unless they originate within a few millimeters of the entrance. The pressure in the system was maintained sufficiently low for these experiments that <0.01 ion pair could be formed by each 23-Mev proton between the target and the back of the Faraday cup and <0.001 ion pair per proton could be formed sufficiently near to the Faraday cup entrance that either member of the pair could traverse the

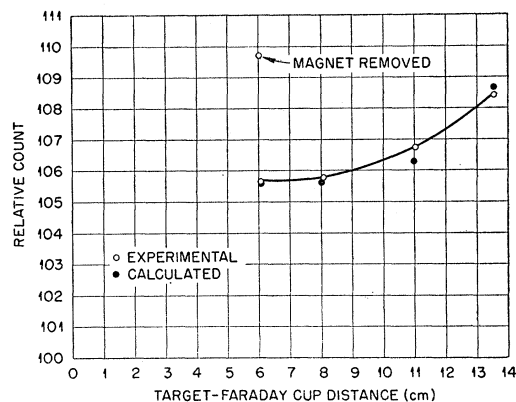


FIG. 2. Relative fission fragment count vs target-Faraday cup distance. These data show the adequacy of the experimental arrangement for reducing the effects of secondary electrons and multiple scattering.

entrance in the presence of the field of the permanent magnet. A movable section of the Faraday cup allows the target-to-Faraday cup distance to be varied, and hence the solid angle subtended by the latter. The relative fission-fragment count observed for a range of target-to-Faraday cup distances is shown in Fig. 2. The calculated curve was computed by use of an approximation method²¹ based on the Molière theory of multiple scattering. It is seen that over a reasonable range of target-to-Faraday cup distance, the relative count does not change appreciably. The datum point obtained with the magnet removed demonstrates the effect of secondary electrons from the target that enter the Faraday cup and hence the need for the magnet.

Since fission fragments from proton fission of uranium are not emitted isotropically, a precision measurement of the number of fission fragments emitted at one angular position is not sufficient for a determination of the fission cross section. The form of the angular distribution and the magnitude of the anisotropies (averaged over the full range of masses) of fission fragments were investigated. For these measurements, the plated targets and a 24-in. diam scattering chamber were used.

The chamber²² consists of two cylindrical parts separated by an O-ring seal and ball bearing assembly. The lower cylinder is stationary; the top cylinder can be rotated (an electric motor and chain drive are used) while the scattering chamber vacuum is maintained. The proton beam enters the chamber through a horizontal pipe near the top of the lower cylinder. There are several flanged circular ports for particle detectors, etc., in the wall of the top cylinder. The flanges are inclined so that the axis of each port intersects the proton beam at the target position. A machined scale on the lower cylinder serves to indicate the angular

¹⁹ The plated uranium targets were prepared and the uranium thicknesses determined by G. S. Petit of the Uranium Measurements Department of the Oak Ridge Gaseous Diffusion Plant.

²⁰ C. B. Fulmer, Phys. Rev. **108**, 1113 (1957).

²¹ W. C. Dickinson and D. C. Dodder, Rev. Sci. Instr. **24**, 428 (1953).

²² The scattering chamber was designed in collaboration with B. L. Cohen, J. E. Mann, and M. B. Marshall.

position of the top cylinder and hence of the particle detector. There are several ports located in the lower cylinder for particle detectors, electrical leads, etc.

For the proton elastic scattering experiments, the incident proton beam is defined by a $\frac{1}{8}$ -in. diam collimator, passes through the target and thence to a Faraday cup, located inside the scattering chamber. The Faraday cup and a stationary scintillation detector, which counts protons elastically scattered from the target, are used to monitor the beam. For obtaining data at angles smaller than ~ 20 deg, the Faraday cup is removed, and the scintillation detector, which is previously calibrated with the Faraday cup for the target being used, serves as the beam monitor.

Self-supporting 0.001-in. thick targets of metallic U^{238} (99.7% isotopic purity) and U^{235} (93% isotopic purity) were used for measurement of proton elastic scattering, (p,p') , (p,d) , (p,t) , and (p,α) reaction cross sections.

A $\frac{1}{8}$ -in. diam collimator for the outgoing particles defined the counting geometry of the detector for the proton elastic scattering experiments. A $\frac{1}{4}$ -in. diam collimator was used for the (p,p') , (p,d) , (p,t) , and (p,α) experiments. The detector consisted of a 0.1-in. thick CsI(Tl) scintillation crystal and photomultiplier tube; pulse-height analysis was used to distinguish the pulses due to elastically scattered protons from those due to background radiations. The energy resolution (defined here as full width at half maximum) of the CsI(Tl) scintillation detector was $\sim 4\%$ for 22-Mev protons. The results were checked with another scintillation detector which used a NaI(Tl) crystal (energy resolution for protons was $\sim 2\%$); the better resolution detector yielded measurements that are in good agreement with those obtained with the CsI(Tl) detector.

Elastic scattering cross sections were measured for the U^{235} and U^{238} targets at intervals of ~ 5 deg over the angular range of 9 deg–171 deg; two complete sets of data were obtained to test the reproducibility of the measurements.

For measurements of proton inelastic scattering cross sections, the U^{235} and U^{238} targets were carefully polished to remove the uranium oxide coat that had formed on the surfaces of the metal foils.

The detector used for (p,p') , (p,d) , (p,t) , and (p,α) reaction cross section measurements consists of a proportional counter-scintillation counter telescope. The detector was used with a particle identification system²³ which can be adjusted to select pulses from a single type of particle to trigger a coincidence gate on the twenty-channel pulse-height analyzer which measures the scintillator pulse-height spectrum. Thus background pulses are eliminated from the energy spectra data. The (p,d) angular distribution data were checked by pulse-height analysis of the output pulses from the particle identification system; triton and alpha-particle pulses

were simultaneously counted by the 20-channel pulse-height analyzer. Approximate measurements of the particle energy distributions were made by displaying the particle identification system pulses on the screen of a cathode-ray oscilloscope and making time-exposure photographs of the screen. This type of display served principally, however, as a qualitative indication to guide the experiment.

RESULTS AND DISCUSSION

(1) Proton Elastic Scattering

The differential elastic scattering cross sections for 22.8-Mev protons on U^{235} and U^{238} are shown in Fig. 3. The same data are shown again in Fig. 4 as the ratio of the cross sections to the Rutherford scattering cross

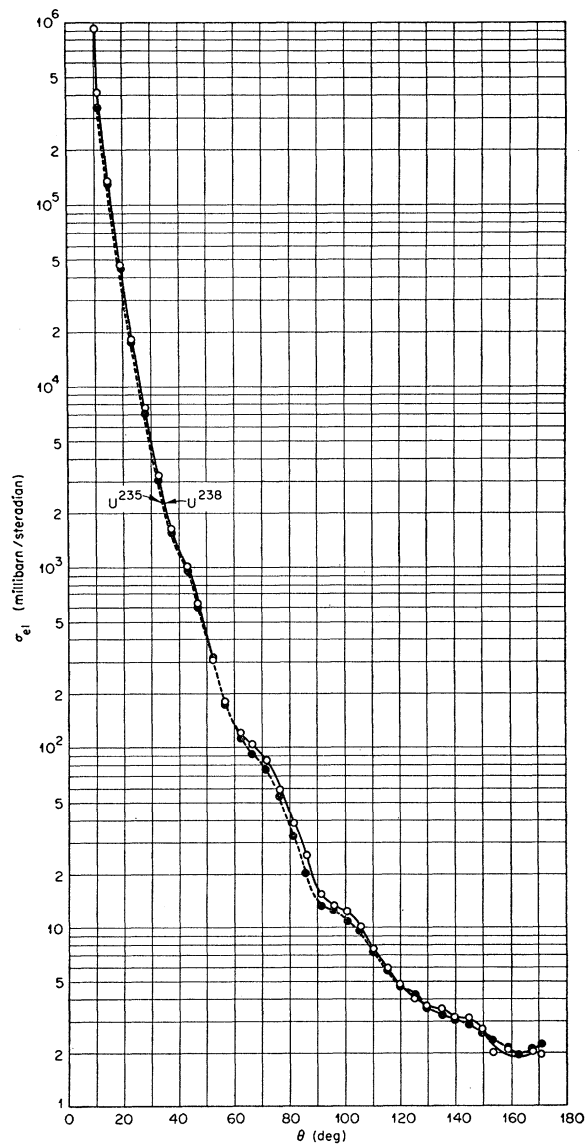


FIG. 3. Differential elastic scattering cross sections for 22.8-Mev protons on U^{235} and U^{238} .

²³ C. D. Goodman and J. B. Ball (to be published).

section to emphasize the details of the angular distributions. The data represent the average of two complete runs. The counting statistics allow standard deviations of $\pm 3\%$ or less in the angular range of 30 deg–140 deg and $\pm 8\%$ or less for the remainder of the data. The variation of data from different runs, that occurred several weeks apart, was less than 10% except at angles < 30 deg and > 150 deg. However, the data contain contributions of inelastically scattered protons that leave the nuclei in low-energy excited states that are not resolved from the pulse-height peak of elastically scattered protons.

The general features of the data are consistent with the pattern of angular distributions of 22-Mev protons elastically scattered by various elements from Be to Th as observed by Cohen and Neidigh,²⁴ i.e., the maxima and minima in the angular distributions occur at positions that could be extrapolated from the earlier data. There are some variations in absolute magnitude of the scattering cross sections for the two isotopes at certain angular regions, e.g., 60 deg–100 deg. These may be associated with the different spins of the two isotopes or possibly with details of the nuclear potential. For instance, Green has suggested²⁵ that there is an $(N-Z)/A$ dependence of the depth of the real nuclear potential.

(2) Fission Cross Sections

(a) The following fission cross sections for 22.8-Mev protons on uranium isotopes were measured by counting fission fragments emitted at 90-deg from the proton beam:

$$\text{for } U^{233}, \sigma(p, \text{fission}) = 1.20 \pm 0.06 \text{ barns};$$

$$\text{for } U^{235}, \sigma(p, \text{fission}) = 1.20 \pm 0.05 \text{ barns};$$

$$\text{for } U^{238}, \sigma(p, \text{fission}) = 1.14 \pm 0.04 \text{ barns}.$$

The data were obtained with several target specimens of different thicknesses and repeated on subsequent

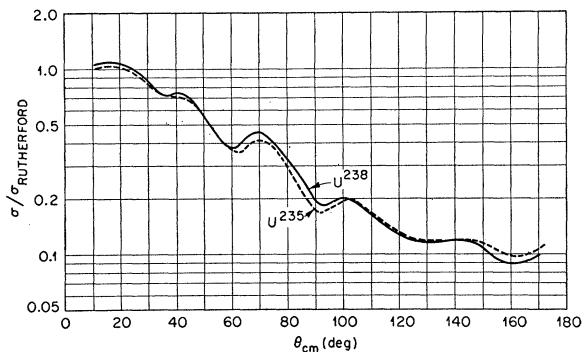


FIG. 4. Differential elastic scattering cross sections for 22.8-Mev protons on U^{235} and U^{238} plotted as ratios to the Rutherford scattering cross sections.

²⁴ B. L. Cohen and R. V. Neidigh, Phys. Rev. **93**, 282 (1954).

²⁵ A. E. S. Green (private communication); A. E. S. Green and P. C. Sood, Phys. Rev. **111**, 1147 (1958).

runs. The uncertainties shown are the standard deviations of all the data obtained. A test showed that the fission rate of a U^{235} target due to neutrons in the scattering chamber is less than 0.5% of the fission rate produced by protons when the target is exposed to the beam used for these experiments.

(b) The angular distributions of fission fragments were investigated. The relation $I(\theta) = a + b \cos^2\theta$ [$I(\theta)$ is the relative intensity observed at angle θ from the proton beam] was checked and found to hold for the entire mass spectrum of fragments as well as for single mass fragments.²⁶ The following anisotropies were observed:

$$\text{for } U^{233}, (b/a) = 0.23 \pm 0.04;$$

$$\text{for } U^{235}, (b/a) = 0.21 \pm 0.03;$$

$$\text{for } U^{238}, (b/a) = 0.22 \pm 0.02.$$

The values obtained here are larger than those observed earlier for single mass fragments.²⁷ However, the sensitivity of total fission cross sections to anisotropy values is not large. The total cross section for the $(p, \text{fission})$ reaction can be written as $4\pi a [1 + \frac{1}{3}(b/a)]$, where $4\pi a$ is the value obtained from measurements with the detector at 90 deg. Thus the discrepancy between these and earlier anisotropy measurements is not a large source of error.

From the combined results of (a) and (b) the fission cross sections are

$$\text{for } U^{233}, \sigma(p, \text{fission}) = 1.29 \pm 0.07 \text{ barns};$$

$$\text{for } U^{235}, \sigma(p, \text{fission}) = 1.28 \pm 0.06 \text{ barns};$$

$$\text{for } U^{238}, \sigma(p, \text{fission}) = 1.22 \pm 0.05 \text{ barns}.$$

To be more precise, the above values are $\sigma(p, xn_f)$ values. The prediction of some theories of nuclear fission that the probability of fission increases with (Z^2/A) is not contradicted here; no experimental distinction is made between fission before and after one or more neutrons are boiled off the compound nucleus. The combined probability of fission of compound nuclei, formed from U^{233} , U^{235} , and U^{238} nuclei and 23-Mev protons before neutron emission lowers the excitation energy below the fission threshold, was computed using Huizenga's values of Γ_n/Γ_f vs mass number.²⁸ For each of the three nuclei, the combined probabilities are ~ 0.98 for cases where the first particle is emitted with low energy. This is for compound nucleus reactions and does not include (p, p') , (p, d) , or any other direct-interaction reactions.

²⁶ Cohen, Jones, McCormick, and Ferrell, Phys. Rev. **94**, 625 (1954).

²⁷ Cohen, Ferrell-Bryan, Coombe, and Hullings, Phys. Rev. **98**, 685 (1955).

²⁸ J. R. Huizenga, Proceedings of the Conference on Reactions Between Complex Nuclei [Oak Ridge National Laboratory Report ORNL-2606, 1958 (unpublished)].

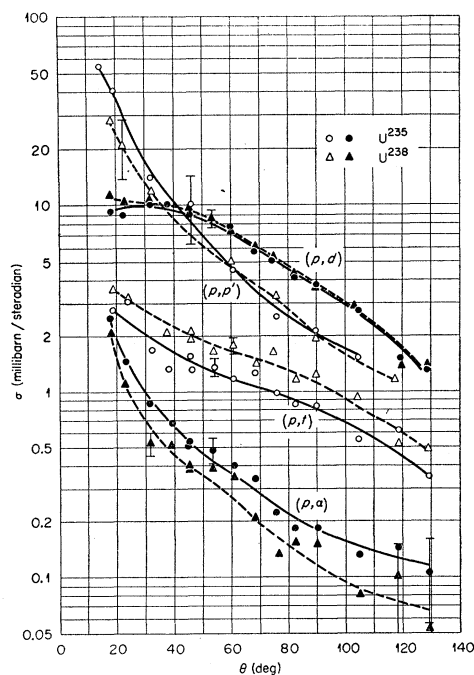


FIG. 5. Differential (p,p') , (p,d) , (p,t) , and (p,α) reaction cross sections for 22.2-Mev protons on U^{235} and U^{238} .

(3) (p,d) Reaction Cross Sections

The angular distributions of observed differential (p,d) reaction cross sections for 22.2-Mev²⁹ protons on U^{235} and U^{238} are shown in Fig. 5. Probable errors are shown for typical data points. The particle identification system used for the experiment insured that all the particles counted were deuterons. The energy spectra of the deuterons extend from ~ 8 Mev to ~ 18 Mev and are peaked at ~ 16 Mev.

(4) (p,t) Reaction Cross Sections

The angular distributions of observed (p,t) reaction cross sections for 22.2-Mev protons on U^{235} and U^{238} are shown in Fig. 5. The data were all obtained by pulse-height analysis of the particle identification system output pulses. The energy distributions of the tritons, as determined by photographs of oscilloscope displays which are discussed above, are approximately the same as that of the deuterons.

(5) (p,α) Reaction Cross Sections

The angular distributions of (p,α) reaction cross sections for 22.2-Mev protons on U^{235} and U^{238} are shown in Fig. 5. The data were all obtained in the same manner as the (p,t) data. The large spread of alpha-particle energy loss in the thick targets used (~ 60

²⁹ These measurements were made somewhat later than the earlier ones. During the interval, repairs were made on the cyclotron with the result that the spectrum of the external beam is peaked at 22.2 Mev rather than 22.8 Mev.

mg/cm²), and the energy loss of the alpha-particles in traversing the proportional counter make the energy distribution determinations from the oscilloscope display photographs rather inaccurate. Qualitatively the spectra are similar, however, to those previously observed for Pt and Au.³⁰ The strongly forward-peaked angular distributions are also very similar to those observed for (p,α) reactions in Pt and Au.

(6) Proton Inelastic Scattering

The cross section for inelastic scattering of 22.2-Mev protons by U^{235} and U^{238} was measured over an angular range of 19 deg–120 deg for Q values extending to -7 Mev which is the fission activation energy for these uranium isotopes. The pulse-height spectra observed at a few angular positions are shown in Fig. 6. A pulse-height spectrum obtained with the scintillation detector at 0-deg position, the target removed, and the ion source of the cyclotron turned off is also shown in Fig. 6; this spectrum contains pulses below the principal peak. These could result from low-energy protons due to slit scattering, etc., and from proton-induced nuclear reactions in the scintillation crystal. The inelastic scattering data obtained at forward angles were

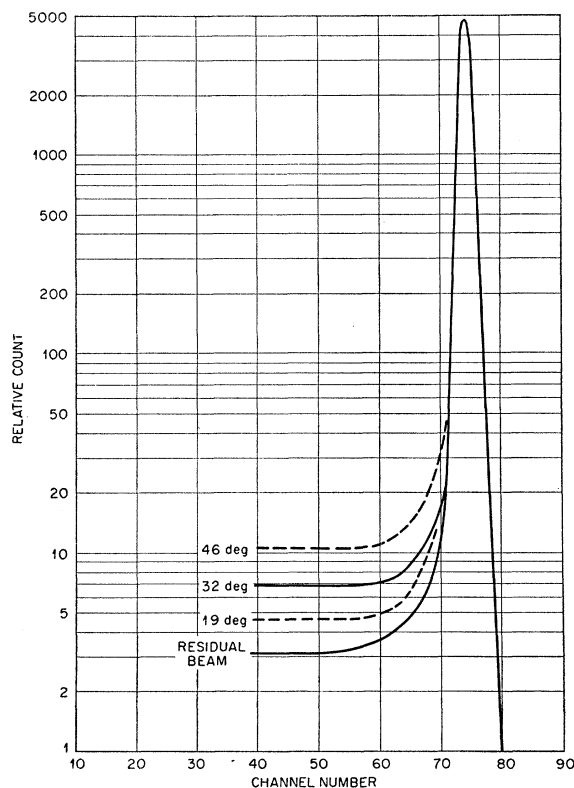


FIG. 6. Pulse-height distributions for protons observed at 0-deg and at other angular positions. The peaks are normalized to show the magnitude of the corrections that were made for pulse-height contamination before the (p,p') cross sections were computed.

³⁰ C. B. Fulmer and B. L. Cohen, Phys. Rev. **112**, 1672 (1958).

corrected for this contamination of the pulse-height spectra before the (p,p') cross sections were computed.

The (p,p') cross section values for 22.2-Mev protons on U^{235} and U^{238} with Q values extending to -7 Mev are shown in Fig. 5. The data do not include contributions from scattering events that leave the residual nucleus in low levels (up to ~ 500 kev) of excitation which are not resolved from the elastic peak. When averaged over all angles, the (p,p') cross section is 65 ± 20 mb for U^{238} and 68 ± 25 mb for U^{235} .

(7) Other Reactions

Cross sections for (p,xn) reactions in U^{238} have been previously investigated.¹⁸ It was found that the $(p,3n)$ reaction is the predominant (p,xn) reaction (without subsequent fission) for 21.5-Mev protons. The measured absolute value at that energy is 32 ± 13 mb. Other (p,xn) reactions were found to be much smaller.

Usually one would need to include contributions for (p,γ) reactions in experimental determinations of total reaction cross sections. However, if the fission cross section is a large part of the total reaction cross section, (p,γ) reactions occur with very small cross sections; for instance, the (p,γ) cross section for 23-Mev protons on Bi^{209} is ~ 0.2 mb.³¹

The results discussed above, of various parts of the total reaction cross sections for protons on uranium isotopes, are summarized in Table I. Although a self-supporting target of U^{238} was not available for measuring the proton elastic scattering, (p,p') , (p,d) , (p,t) , and (p,α) cross sections of that isotope, it is well known that for heavy elements, they vary very slowly with A -values. The combined total reaction cross sections

TABLE I. Reaction cross sections for 22.8-Mev protons on uranium isotopes. All cross sections are in barns.

Reaction	U^{238}	U^{235}	U^{238}
(p,f)	1.29 ± 0.07	1.28 ± 0.06	1.22 ± 0.05
(p,xn)	0.035^a	0.035^a	0.35 ± 15^b
(p,d)	0.050^a	0.050 ± 0.005	0.050 ± 0.005
(p,t)	0.013^a	0.011 ± 0.004	0.013 ± 0.004
(p,α)	0.004^a	0.004 ± 0.001	0.003 ± 0.001
(p,p')	0.065^a	0.068 ± 0.025	0.065 ± 0.020
Total	1.43 ± 0.10	1.44 ± 0.10	1.39 ± 0.10

^a These cross sections are inferred from the data for other uranium isotopes.

^b See reference 18.

given in Table I include allowances in the uncertainties for low-lying levels excited in (p,p') reactions. No allowance is made for rotational levels, however; for neutrons the cross sections for excitation of these levels are rather large.³² However, rotational levels are predominantly excited in elongated nuclei. Although it is likely that uranium nuclei are elongated, the optical model analysis of elastic scattering data employs a spherical nuclear model and hence the reaction cross sections thus obtained do not include contributions due to nuclear eccentricity.

ACKNOWLEDGMENTS

The author gratefully acknowledges the interest and assistance of B. L. Cohen, C. D. Goodman, and J. B. Ball in various phases of the experimental work, the assistance of E. L. Olson in electronic problems, and of M. B. Marshall, C. L. Viar, and F. A. DiCarlo in various aspects of cyclotron operation and proton beam control. The support and encouragement of R. S. Livingston are also gratefully acknowledged.

³¹ E. L. Kelley, University of California Radiation Laboratory Report UCRL-1044, 1952 (unpublished).

³² Chase, Willets, and Edmonds, Phys. Rev. **110**, 1080 (1958).